SYNTHESIS AND CHARACTERIZATION OF TITANIUM-ZINC NANOPARTICLES

HIMA BINDU G[1], MANOHARI J[2], VAMSI KUMAR Y[3]
Department of Engineering Chemistry,
AUCE (A), Andhra University,
Visakhapatnam, India- 530003

Abstract

The present paper focused on preparation and characterization of nanoparticles of Titanium and Zinc. Material scientists and engineers have made significant developments in the improvement of methods of synthesis of nanomaterial solids. In this work, Ti & Zn nanocomposite were readily synthesized through sol-gel method using Titaniumdioxide & Zincsulphate as precursors. The prepared nanoparticles were characterized using FT-IR, XRD, UV-visible spectroscopic techniques. Experimental statistics showed that the photocatalyst (Ti-Zn) is synthesized by a low cost method and had the least grain size and its photocatalytic performance was the best. The aim of this research was to find a simple route to prepare pure Ti & Zn nanoparticles via sol-gel method and characterize the final product using several techniques.

Keywords: Pure Ti & Zn nanoparticles, Sol-gel, FT-IR, XRD and UV-visible spectroscopy.

I. Introduction

Nano is an advanced technology which in recent years has numerous applications in different fields such as industry, biotechnology, energy, environment etc. Nano sized particles of semiconductor materials have gained much more interest in recent years due to their desirable properties and applications in different areas such as catalysts,[1] sensors,[2] photoelectron devices,[3,4] highly functional and effective devices.[5] Pure nanoparticles have a great advantage to apply a catalytic reaction process due to their large surface area hence have ability to adsorb small molecules and high catalytic activity.[6] These are expected to play a crucial role in water purification.[7] In recent years, nano sized particles wide applications in other modern scientific and technological field because of its wide direct band gap, strong excitonic binding energy and promising application for UV-laser with low threshold, field emission array[8,9] surficial acoustic device[10] and transistor and biosensor[11] in nanoscales. Titanium exhibits excellent physical and chemical properties. It has a good biocompatibility and bio integration with the human body. Pure Titanium 99.9% is a preferred material for medical application. The chemical process deals with the photocatalysts like pure nano titanium & nano zinc, mediated degradation of the industrials waste water. Recently, Xiaobo and Samuel reviewed the broad applications of titanium dioxide as a photocatalyst. Several methods have been used successfully in the synthesis of pure nano titanium & nano zinc materials for medical application. Reduction of transition metal salts is the oldest, easiest and still a widely used method for the preparation of metal nanoparticles. Sol-gel method can be a simple method as it requires low temperature and controllable final product properties.[12-14] In this method materials undergo hydrolysis and polycondensation processes to form the sol and then gel will be formed after aging or gelation and eventually become solid crystals after drying.

II. Synthesis of photocatalyst (Ti:Zn) (sol-gel processing)

Materials and methods

TiO_2 (AR) (surface area $50m^2/g$), $ZnSO_4.7H_2O$ (AR) (surface area $50m^2/g$), Surfactant (SDS), Ethyl alcohol, Distilled water were used for preparation of various solutions. All chemicals and reagents used in this process are of AR grade fine chemicals.

Procedure

The sol-gel synthesized nano titanium obtained from titanium dioxide (TiO_2) was dissolved in absolute ethanol in terms of a molar ratio of Ti:Ethanol(1:10). Hydrochloric acid was used to adjust the pH2. The above solution was stirred vigorously until a clear solution was obtained, then **s**urfactant (SDS) was dissolved in **e**thanol according to a setting molar ratio and fed into the titanium salt solution slowly (0.5ml/min). Hydrolysis reaction and polymerization took place in this mixture and titanium dioxide solution was formed. After stirring, the solution was aged for 24h, it transformed into white powder. In order to obtain nanoparticles, the gels were dried at 100^0C in an oven for 2h to evaporate water and organic material to the maximum extent. After calcined in muffle furnace at high temperature, for 5h white titanium nanoparticles were obtained. The addition of surfactant sodium dodecyl sulphate (SDS) can influence particle growth, coagulation and flocculation. Therefore, surfactants play an important role in the preparation of other metal oxide nanoparticles.

The sol-gel synthesized nano zinc was obtained from zinc sulphate heptahydrate was dissolved in absolute ethanol in terms of a molar ratio of Zn:Ethanol (1:10). Hydrochloric acid was used to adjust the pH2. The above solution was stirred vigorously until a clear solution was obtained, then **s**urfactant (SDS) was dissolved in **e**thanol according to a setting molar ratio and fed into the zinc salt solution slowly (0.5ml/min). Hydrolysis reaction and polymerization took place in this mixture. After stirring, the solution was aged for 24h, it transformed into white powder. In order to obtain nanoparticles, the gels were dried at 100^0C in an oven for 2h to evaporate water and organic material to the maximum extent. After calcined in muffle furnace at high temperature for 5h white zinc nanoparticles were obtained. The synthesized Ti:Zn nanocomposites were mixed with different weight ratios (0:1, 1:0, 1:1, 2:1, 1:2) in presence of sunlight. Images of nano titanium and nano zinc particles have been shown in **fig 1.**

Fig1: Digital images of (a) Nano titanium particles and (b) Nano zinc particles

III.Characterization

UV DRS

Band gaps were calculated using Single Monochromator UV-2600 (optional ISR-2600Plus, λ up to 1400nm). The measurement of the band gap of materials is important in the semiconductor, nanomaterial and solar industries. The band gap of a material can be determined from its UV absorption spectrum. Band gap is calculated from the equation where λ is the wavelength of the material from the graph.
Eg is the band width to be calculated.

$$Eg = \frac{1240}{\lambda(nm)}$$

The spectrum of all solar electromagnetic radiation striking the Earth's atmosphere spans a range of 100nm to about 1nm
In terms of energy at earth's surface:

52 to 55% infrared (above 750nm)

42 to 43% visible (400 to 750nm)

3 to 5% Ultra violet (below 400nm)

Spectrum	Wavelength (nm) (λ)	Band gap Energy Eg(ev)
Infrared	λ >750	Eg<1.65
Visible	750> λ >400	1.65<Eg<3.10
Ultra violet	λ <400	3.10<Eg

The band gap can be estimated from UV–Visible spectra.

FT-IR analysis

The FT-IR study of the synthesized nano crystal was performed using Frontier IR model FT-IR-8400S. FT-IR is one of the most widely used tools for the detection of functional groups in pure compounds and mixtures. FT-IR spectrometers are mostly used for measurements in the mid and near IR regions. The FT-IR spectroscopy is widely used to study the nature of surface adsorbents in nanoparticles. Since the nanoparticles possess large surface area, the modification of the surface by a suitable adsorbate can generate different properties.

X-Ray Diffractometer

The crystal structure and crystal phase of the prepared pure Ti-Zn nanocomposite samples were examined by the XRD technique. The measured 2-theta range between 20^0 and 80^0 was scanned with the velocity of 2.0000(deg/min). XRD analysis indicates that samples treated at temperatures below 400°C show weakly crystalline phase, which could be rutile-based. If temperature is at

400°C and above, evidence for a two-phase anatase and rutile structure can be distinguished. And also based on the peak widths, the crystallite size for anatase is much larger than for rutile.

IV. **Results and Discussions**

Band gap calculation

The optical properties of pure Ti:Zn nanocomposites were evaluated by UV-Diffuse Reflectance Spectroscopy. Before calcination of Ti-Zn nanocomposites shows the λ_{max} at 310nm and the calculated band gap was found to be 4.0eV, which **was** shown in **fig 2(a)**. After calcination Ti-Zn nanocomposites shows a λ_{max} at 320nm and the band gap was found to be 3.8eV, which **was** shown in **fig 2(b)**. The band gap was tuned from 4.0 eV to 3.8eV by raising the temperature.

The band gap of a solid and the wavelength of light that is reflected by it are related to one another via the Planck-Einstein Relation, which is stated below. E_g is the gap energy of the band gap in joules, h is Planck's constant (6.63×10^{-34} J **s**), ν is frequency in hertz.

$$E_g = h\nu = \frac{hc}{\lambda}$$

From the plot of absorbance vs wavelength (λ), wavelength of the material is measured and band gap is calculated from the equation, where λ is the wavelength of the material from the graph. E_g is the bandwidth to be calculated

$$Eg = \frac{1240}{\lambda(nm)}$$

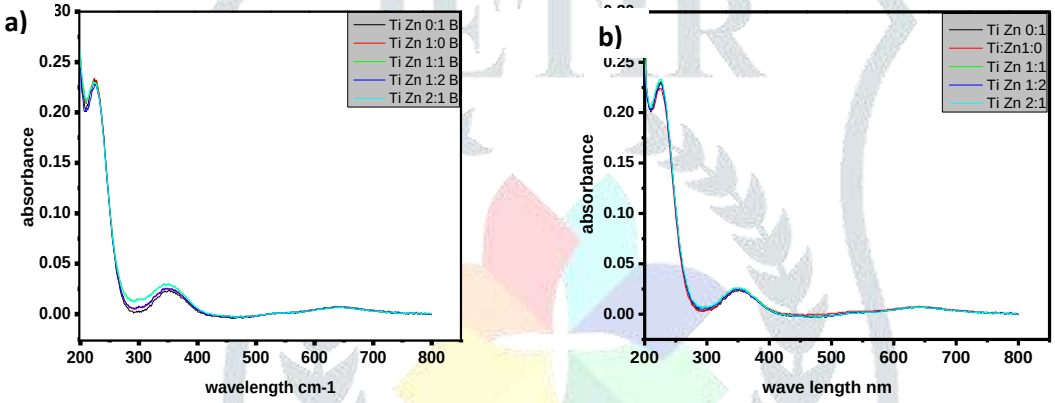

Fig 2: Band gap spectrum of Ti:Zn nanocomposites (a) Before calcination and (b) After calcination

FT-IR of metal composites

The **FT-IR** spectroscopy of the Ti:Zn nanocomposites before and after calcination treatment is shown in **fig 3**. It is believed that the broad peak at 3400cm^{-1} and the peak at 1621cm^{-1} correspond to the hydroxyl groups and surface-adsorbed water respectively. The peaks in the range of 1400-1500cm^{-1} corresponds to the C=O bonds. The absorbed band at 1626cm-1 is assigned O-H bending vibration.

The main peak at 400–700cm^{-1} was attributed to Ti-O stretching and Ti-O-Ti bridging stretching modes. Notably, with increasing temperature, the surface-adsorbed water and hydroxyl groups decreased slightly. This was due to the decrease of specific surface areas and pore volume, which caused the reduction of the adsorbed water. According to our previous study, the hydroxyl groups on the surface of samples contribute to enhancement of the photocatalytic activity, because they can interact with photogenerated holes, which gives better charge transfer and inhibits the recombination of electron-hole pairs.

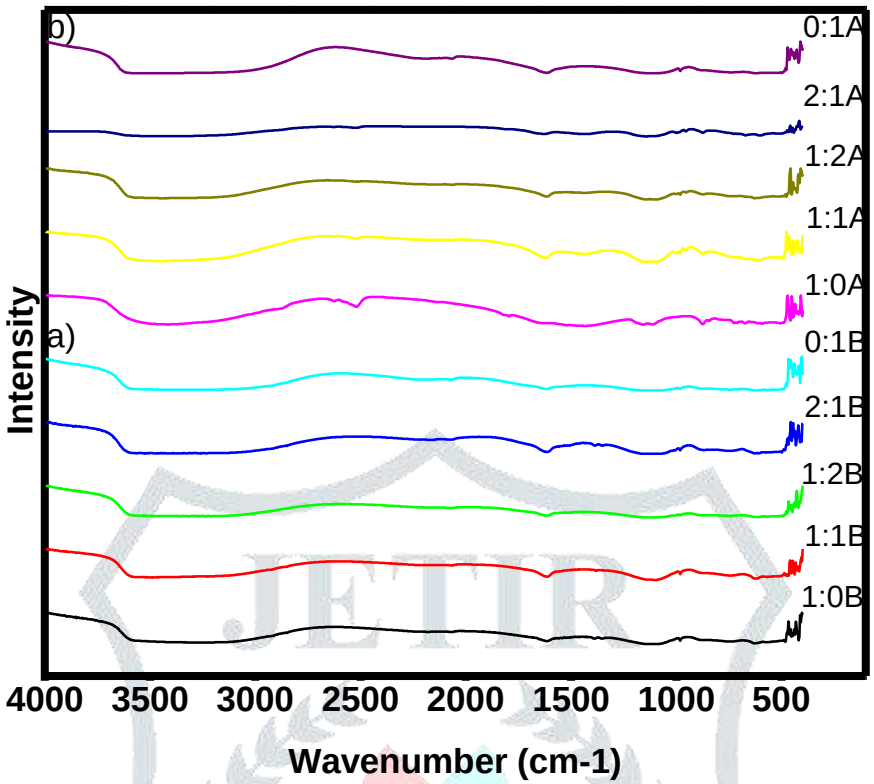

Fig 3: FT-IR spectra of the Ti:Zn nanocomposite powder (a) Before and (b) after calcination

XRD of metal composite

XRD analysis determined the phase's presence in nanopowder. The grain size and phase of the Ti:Zn nanocomposites obtained were determined by X-Ray diffraction spectroscopy using (PAN analytical –X'Pert) professional X-ray beam diffractometer with a scan rate velocity of 2.0000 (deg/min). **Fig 4** represents the XRD patterns of Ti:Zn nanocomposite samples before and after calcination. The effect of calcination temperature on phase structures was studied using XRD. The intensity of the peaks increases with calcination temperature, indicating increased crystallinity. Further observation shows that with increasing calcination temperature to 400^{O}C the intensity of both anatase and rutile peaks gradually increases, indicating an enhancement of crystallization. Therefore, the calcination temperature obviously influences the crystallization and phase composition of the Ti:Zn powders. High calcination temperature results in the phase transformation from anatase to rutile. Usually, phase transformation is accompanied with crystal growth. As the calcination temperature is raised, XRD reflections corresponding to both the anatase and rutile phase become narrower, which indicates the increase of crystallite size. A significant increase in crystallite size is observed for the sample calcined at 400°C. The particles sizes in the samples were in the range of 13.7-30.8nm when calcined at 400°C. The particle size calculated using Debye-Scherrer formula $D = 0.941/(P\cos\theta)$,

Where X the X-ray wavelength,

P the peak width of half-maximum, and

θ is the Bragg's diffraction angle.

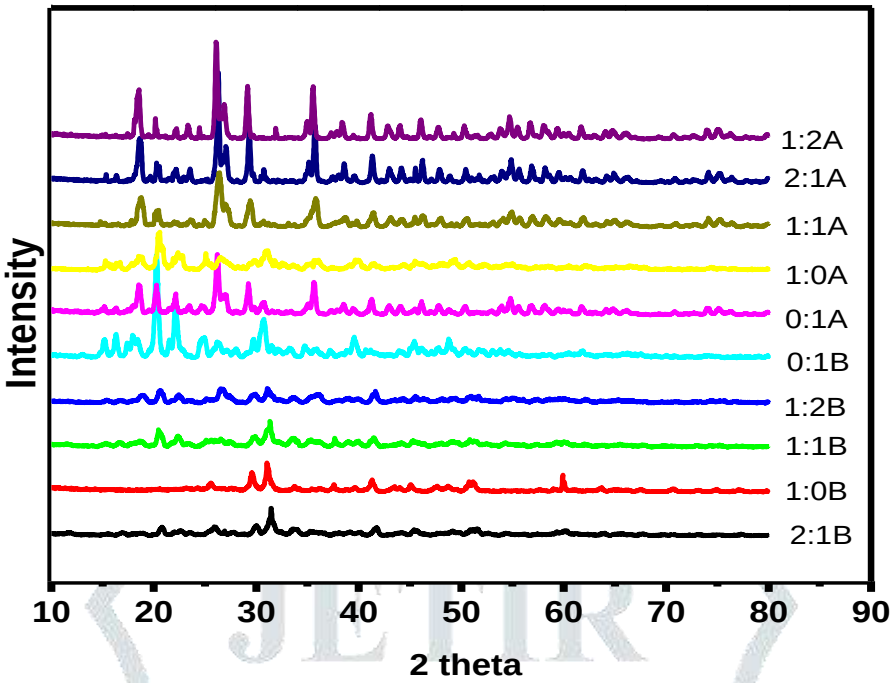

Fig 4: XRD patterns of Ti:Zn nanocomposite samples before and after calcination.

IV. **Conclusion**

2θ

The synthesized material was characterized using XRD, FTIR, UV–visible spectroscopic techniques. The average particle size was found to be < 30nm for Ti/Zn nanoparticles (1:0, 1:2, 1:1, 2:1 and 0:1) calcined at 400^0C. The optical band gap was calculated using absorption spectra ranging from 4.0eV to 3.8eV by raising the temperature.

V. **References**

1. Joshi, S. S, Patil, P. R, Naimase, M. S, Bakare, P. P. 2006. Role of ligands in the formation, phase stabilization, structural and magnetic properties of α-Fe2O3 nanoparticles. J. Nanopart. Res, 5: 635–643.
2. Cheng, X. L, Zhao, H, Huo, L. H, Gao, S, Zhao, J. G, 2004. ZnO nanoparticulate thin film: preparation, characterization and gas-sensing properties. Sens.Actuators B, 102: 248–252.
3. Lee, S. Y, Shim, E. S, Kang, H. S, Pang, S. S. 2005. Fabrication of ZnO thin film diode using laser annealing. Thin Solid Films, 437: 31–34.
4. Wang, Z. L, Kong XY, Ding Y. Gao P, Hughes, W. L. 2004. Semiconducting and piezoelectric oxide nanostructures induced by polar surfaces. Adv. Funct.Mater, 14: 943–956.
5. Huang, Y. H, Zang, Y, Liu, L, Fan, S. S, Wei, Y. and He, J. 2006. Controlled synthesis and field emission properties of ZnO nanostructures with differentmorphologies. J. Nanosci. Nanotechnol, 6: 787–790.
6. Chen, J. C, Tang, C. T. 2007. Preparation and application of granular ZnO/Al2O3 catalyst for the removal of hazardous trichloroethylene. J. Hazard. Mater. 142: 88–96.
7. Stoimenov, P. K, Klinger, R. L, Marchin, G. L. and Klabunde, K. J. 2002. Metal oxide nanoparticles as bactericidal agents. Langmuir. 18: 6679-6686.
8. Xu, C. X, Sun, X. W. 2003. Field emission from zinc oxide nanopins. Applied Physics Letters, 83: 3806–3808.
9. Xu, C. X, Sun, X. W, Chen, B. J. 2004. Field emission from gallium-doped zinc oxide nanofiber array. Applied Physics Letters, 84:1540–1542.
10. Zhao, M. H, Wang, Z. L. and Mao, S. X. 2004. Piezoelectric characterization individual zinc oxide nanobelt probed by piezoresponse force microscope. Nano Letters, 4: 587–590.
11. Arnold, M. S, Avouris, P, Pan, Z. W. and Wang, Z. L. 2003. Field-effect transistors based on single semiconducting oxide nanobelts. Journal of Physical Chemistry B, 107: 659–663.
12. Campbell, L. K, Na, B. K. and Ko, E. I. 1992. "Synthesis and characterization of titania aerogels," *Chemistry of Materials*, 4: 1329–1333.
13. Prasada Rao, A. V, Robin, A. I. and Komarneni, S. 1996. "Bismuth titanate from nanocomposite and sol-gel processes," *MaterialsLetters*, 28: 469–473.
14. Vieira, D. F. and Pawlicka, A. 2010. "Optimization of performances of gelatin/LiBF4-based polymer electrolytes by plasticizing effects," *Electrochimica Acta*, 55: 1489–1494.